β-amyloid Aggregation | Hot Paper

DOI: 10.1002/ange.201311106

The Molecular Structure of Alzheimer β-Amyloid Fibrils Formed in the Presence of Phospholipid Vesicles**

*Zheng Niu, Weijing Zhao, Zhengfeng Zhang, Fanshu Xiao, Xinqi Tang, and Jun Yang**

Abstract: *β-amyloid (Aβ) fibrils are the major species involved in Alzheimer's disease (AD). An atomic-resolution molecular structure of Aβ40 fibrils formed in the presence of lipid vesicles was obtained by using magic angle spinning (MAS) solid-state NMR spectroscopy. The fibril structures formed in the presence of the lipid vesicles are remarkably different from those formed in solution. These results provide insights into the molecular mechanism of Aβ aggregation in the presence of lipid vesicles.*

Alzheimer's disease (AD) is characterized by the presence of neuritic plaques and neurofibrillary tangles in the brain. β-amyloid peptide (Aβ) fibrils are the major components of amyloid plaques. A variety of morphologies of Aβ fibrils have been detected by electron microscopy (EM). Previous studies have demonstrated that the toxicity of Aβ fibrils is associated with their morphology and molecular structure.[1] Studying fibril structures of diverse morphologies and under different formation conditions is thus important to gain structural insights into AD. Structural models of the Aβ fibrils formed in solution with various morphologies have been revealed by solid-state NMR and EM.[2–5] However, under biological conditions, the interactions between Aβ and membranes play an important role in the aggregation of Aβ[6–9] because Aβ is generated from the cleaving of the amyloid precursor protein (APP) and is likely bound to the neuronal membrane surface. Moreover, Aβ aggregates probably exert their toxic action through distortion of the neuronal membrane or alteration of the permeability of the neuronal membrane through the formation of ion channels.[10,11] In spite of the importance, in terms of neuropathology, of Aβ fibrillization in the presence of the membrane, atomic-resolution structural information is lacking.

Solid-state magic angle spinning (MAS) NMR spectroscopy is a powerful tool for providing atomic-resolution structures for insoluble and uncrystallizable amyloid fibrils.[12–19] In the past 15 years, MAS NMR has led to encouraging structural insights into the mechanism of Aβ fibrillization in Alzheimer's disease.[3,5,20–25] However, the broad linewidths typically associated with MAS NMR signals of the fibrils hamper structural characterization by using [^{13}C,^{15}N]-labeled samples and multidimensional MAS NMR experiments. Generally, a number of fibril samples of chemically synthesized Aβ peptides with site-specific labeling are used in MAS NMR experiments. In this study, highly ordered Aβ40 fibril samples were obtained through the fibrillization of recombinantly expressed Aβ40 peptides. Such highly ordered [^{13}C,^{15}N]-labeled fibril samples significantly improve MAS NMR spectral resolution, thus permitting detailed

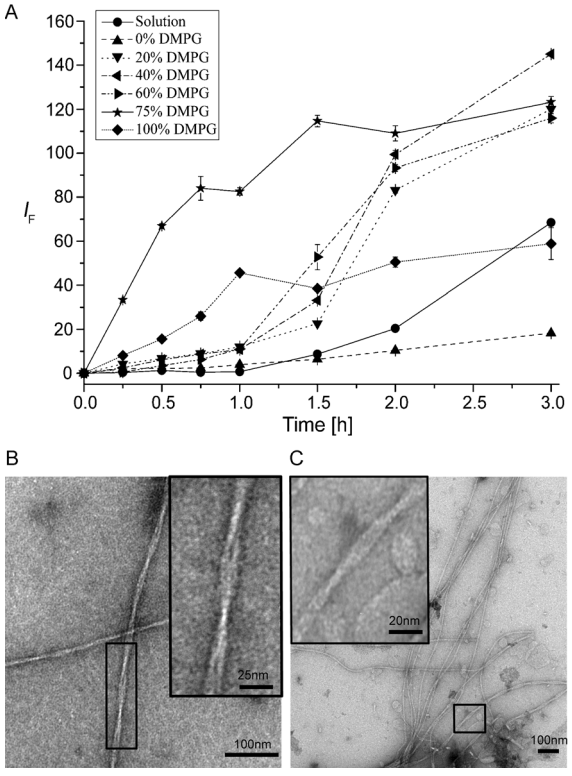

Figure 1. A) Thioflavin T (ThT) fluorescence measured during the aggregation of 50 μM Aβ40 peptide in solution and in the presence of the DMPC/DMPG vesicles with different percentages of the anionic lipid DMPG. TEM images are shown for 50 μM Aβ40 peptide after incubation in solution for 96 h (B) or in the presence of DMPC/DMPG (1:3 molar ratio) vesicles for 2 h (C). Fluorescence intensities were measured at λ_{ex} = 440 nm, λ_{em} = 485 nm. The error bars in (A) are standard deviations of three measurements. Points with no visible error bars represent measurements with tiny variance. DMPC = 1,2-dimyristoyl-*sn*-glycero-3-phosphocholine, DMPG = 1,2-dimyristoyl-*sn*-glycero-3-phosphoglycerol.

[*] Z. Niu,[+] W. Zhao,[+] Dr. Z. Zhang,[+] Dr. F. Xiao, X. Tang, Prof. J. Yang
Key Laboratory of Magnetic Resonance in Biological Systems, State Key Laboratory of Magnetic Resonance and Atomic and Molecular Physics, Wuhan Center for Magnetic Resonance, Wuhan Institute of Physics and Mathematics, Chinese Academy of Sciences
Wuhan, 430071 (P.R. China)
E-mail: yangjun@wipm.ac.cn

[+] These authors contributed equally to this work.

[**] J.Y. acknowledges a Humboldt Foundation fellowship and Clemens Glaubitz. This work is supported by National Natural Science Foundation of China (21075133, 21173259). We acknowledge Riqiang Fu for reading the manuscript.

Supporting information for this article is available on the WWW under http://dx.doi.org/10.1002/anie.201311106.

resonance assignments and leading to the identification of a novel structural model, which is different from the structures of Aβ40 fibrils formed in solution.

The formation kinetics of amyloid fibrils in solution and in the presence of the DMPC/DMPG lipid vesicles with different percentages of the anionic lipid DMPG were monitored through measuring thioflavin T (ThT) fluorescence (Figure 1 A and Figure S1 in the Supporting Information). The ThT fluorescence data indicate that the fibrillization kinetics of the Aβ40 peptide in the presence of lipid vesicles are significantly influenced by the percentage of the charged lipid DMPG. This result is in good agreement with previous studies.[6,7] The acceleration of aggregation in the presence of charged lipids was evident from negatively stained transmission electron microscopy (TEM). The TEM images of the fibrils harvested from incubation in solution for 96 h (solution fibrils) and in the presence of the DMPC/DMPG (1:3 molar ratio) lipid vesicles for 2 h (lipid fibrils) are shown in Figure 1 B and C, respectively. Both fibrils show various morphologies. One of morphologies of the solution fibrils is "twisted pairs",[3] which is composed of two filaments, each with a width of 4–9 nm, with a twist period of 70 ± 40 nm.

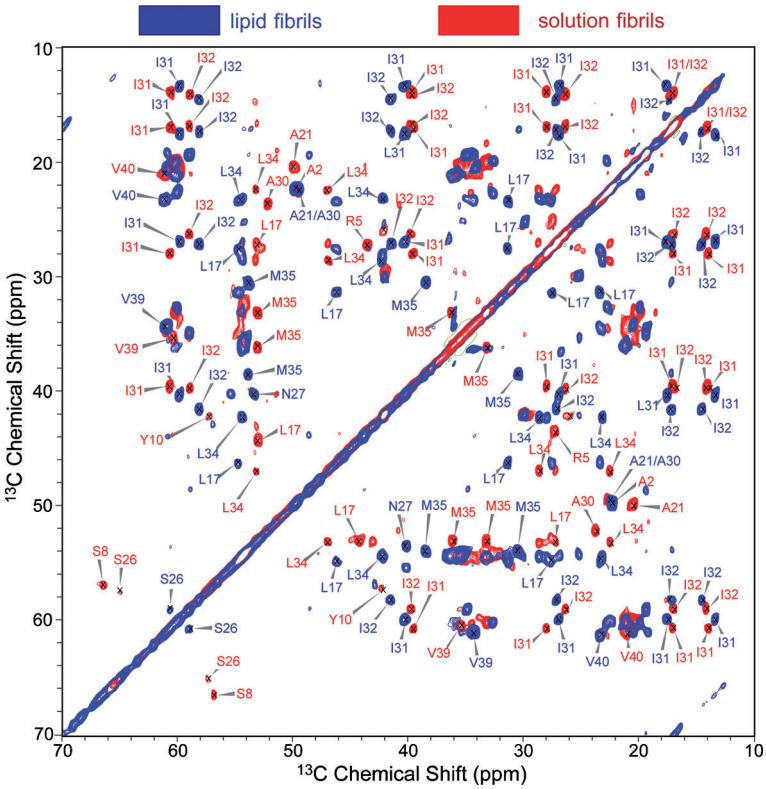

Figure 2. 2D ^{13}C-^{13}C DARR spectra with a 50 ms DARR mixing time of [^{13}C,^{15}N]-labeled Aβ40 fibrils formed in the presence of lipid vesicles (blue) or in solution (red). The spectra were acquired on a 800 MHz NMR spectrometer at 283 K and a 10.672 kHz MAS rate. The marked assignments were based on a set of 3D NCACX, NCOCX, and CONCA experiments.

Both fibrils were characterized by 2D ^{13}C-^{13}C dipolar assisted rotational resonance (DARR) spectra (Figure 2). Typically, ^{13}C linewidths of 50–120 Hz were observed in both 2D ^{13}C-^{13}C correlation spectra, thus indicating a high degree of conformational homogeneity. The linewidths are comparable to those reported by Bertini[4] and Reif et al.[23] In these three studies (including ours), all of the fibril samples were prepared by using recombinantly expressed Aβ40 peptides, thus suggesting that biosynthetic Aβ40 peptides more easily form highly ordered fibrils than those from chemical synthesis. It should be noted that, although the fibrils appear polymorphous in the TEM images, a single set of signals for all residues were observed in 2D ^{13}C-^{13}C correlation spectra, thus indicating only one species for each type of fibril. Superposing the 2D ^{13}C-^{13}C correlation spectra for the lipid fibrils and solution fibrils reveals significant differences in the chemical shifts, thus suggesting a difference in their molecular structures.

To obtain the sequence resonance assignments for both fibrils, we conducted a set of 3D experiments, including 3D NCACX, CONCA, and NCOCX, by using the [^{13}C,^{15}N] Aβ40 fibril samples. Representative 2D strips of these 3D spectra are shown in Figure S2 in the Supporting Information. We obtained complete resonance assignments for residues 16–40 of the lipid fibrils (Table S1 in the Supporting Information). Residues 1–15 were not detected by either dipolar-coupling-based experiments such as CP or the scalar-coupling-based technique INEPT, thus indicating structural disorder or high mobility of the N-terminal segment. By contrast, we were able to assign resonances for 36 residues of the solution fibrils (Table S2). The secondary structures of both types of fibril were analyzed by secondary chemical shifts[26,27] and TALOS+.[28] A comparisons of secondary chemical shifts and predicted secondary structures for the lipid fibrils and solution fibrils are shown in Figure 3 (see also Figures S3 A and S4). These figures all show significant differences between the secondary structures of the lipid fibrils and the solution fibrils. The structural differences were further confirmed by structure calculations.

To characterize the structure of the monomeric unit of the lipid fibrils, we identified intramolecular-distance restraints by using ^{13}C-^{13}C DARR spectra with long mixing times and using a [^{13}C,^{15}N]-labeled sample diluted by natural abundance Aβ40 molecules. A molar ratio of the labeled to natural abundance molecules of 1:3 was used to suppress intermolecular interactions. From a series spectra with DARR mixing times of 50 to 400 ms, we unambiguously assigned a variety of intramolecular restraints. These could be used to define β1–β2 interstrand contact such as V39–L17 and I32–E22 (Figure S5 and Table S4). By using 59 intramolecular-distance restraints and 32 torsion-angle restraints from TALOS predictions, a structural model of the monomeric unit was calculated by Xplor-NIH.[29] In the structure with the lowest total experimental restraint energy (Figure 4), the β2 strand is distorted by a kink at Gly33 and a bend at Gly37–38. It should be noted that we used only "good" predicted TALOS torsion angles as

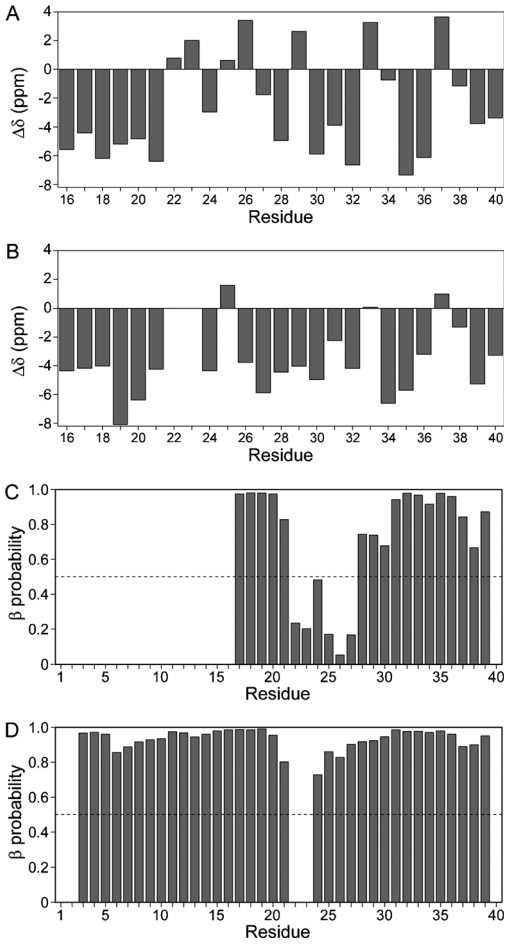

Figure 3. Secondary chemical shifts ($\Delta\delta$) of lipid fibrils (A) and solution fibrils (B). $\Delta\delta$ values were calculated according to Equation 1 in Ref. [27]. The probability of β-strand secondary structure for Aβ40 lipid fibrils (C) and solution fibrils (D) predicted by TALOS+[28] by using MAS NMR chemical-shift assignments. The dashed line indicates a probability of 50%.

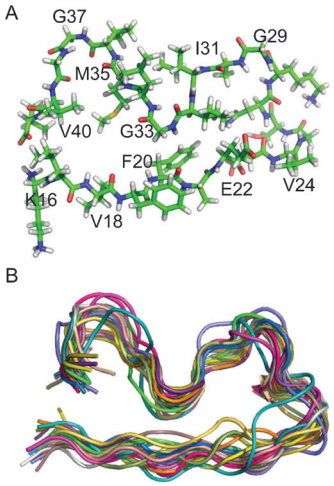

Figure 4. A Structural model of the monomeric unit of Aβ lipid fibrils. A) The structure with the lowest experimental restraint energy in the Xplor-NIH calculations. B) Superposition of the 20 lowest-energy structures (out of 400 calculated structures) with an average backbone RMSD of 2.15 Å.

restraints for the structure calculations and not all of the torsion angles of glycine residues were included. Therefore, the twists in the β2 strand in the calculated structure are not derived from TALOS torsion angles of the glycine residues. The twists in the β2 strand result in nonparallel contact of the β1 and β2 strands (Figure 4). This nonparallel contact pattern of the β1 and β2 strands has also been reported in the fibrils formed in brain tissues.[5] However, the details of the contacts are different. By contrast, non-kinked and parallel β1-strand–turn–β2-strand structures of solution fibrils were reported by Bertini[4] and Tycko et al.[2,3,30] Our MAS NMR data demonstrate that our solution fibrils exhibit similar structure to those reported by Bertini and co-workers.[4] The similarities of the structures are supported by the surprisingly similar 2D NCA and ^{13}C-^{13}C correlation spectra (Figure S6) and the similar secondary chemical shifts (Figure S3B) of these two sets of solution fibrils. Furthermore, we have observed a number of distance restraints for defining β1–β2 interstrand contacts such as F19–L34 (Figure S7) and F19–V36 (Figure S8). These restraints are also reported for Bertini's solution fibrils.

To reveal the organization of the monomeric unit of the lipid fibrils, we assigned intermolecular restraints by comparing the 2D ^{13}C-^{13}C DARR spectra of [^{13}C,^{15}N]-labeled Aβ fibrils diluted or undiluted with natural abundant Aβ molecules. Since the cross peaks in the spectra of the diluted sample belong to intramolecular correlations, cross peaks present in the spectra of the undiluted sample but absent in the spectra of the diluted sample can be assigned to intermolecular correlations. By using this approach, we assigned a number of intermolecular-distance restraints, including V39–G29, V39–A30, V39–I31, G38–I31, and G38–I32 (Figure S9 and Table S5). Since the above restraints are possibly present in three-fold[3] and antiparallel two-fold symmetric models,[2,4] more intermolecular restrains are required to define the organization of the monomeric units, and work in this direction is in progress.

The present study demonstrates that the interaction of Aβ40 peptides with lipids not only influences the aggregation kinetics but also alters the molecular structure of the resulting fibrils. The key observation is that the structure of Aβ lipid fibrils is significantly different from that of solution fibrils. The structure difference can be attributed to the template effect of anionic phospholipids in Aβ40 fibril nucleation. There are two aspects to this effect. Firstly, the two-dimensional membrane matrix provides a different environment from the solution, in which Aβ40 molecules self-associate with relatively few restraints. Secondly, the interactions between Aβ40 and the membrane, especially electrostatic interactions, mediate Aβ40 intramolecular and intermolecular interactions, which are major driving forces of the self-assembly of Aβ40, thus leading to fibrils of a different structure. In recent simulations, electrostatic interactions between anionic lipids and the charged residues of Aβ were observed to destabilize the β-turn-β motif of Aβ40 fibrils and mediate aggregation.[31] Our experimental results are consistent with this study.

In summary, we have characterized the molecular structure of Aβ40 fibrils formed in the presence of lipid vesicles by using [^{13}C,^{15}N]-labeled samples and multidimensional MAS NMR spectroscopy. The structure of the lipid fibrils is distinct from that of solution fibrils. This study not only provides the first structural model of Aβ40 fibrils formed in the presence of the lipid vesicles, but also demonstrates how peptide–lipid interactions influence the fibrillization of the Aβ40 peptide, a process that is closely associated with the pathophysiology of AD.

Experimental Section

Aβ40 peptides were expressed in the BL21 (DE3) PLysS *E. coli* strain and purified by ion-exchange chromatography. To prepare fibrils in solution, lyophilized Aβ40 peptide was dissolved in NaOH (50 mM) and then diluted with NaPi buffer (10 mM pH 7.4) to a final Aβ40 concentration of 50 μM. The pH value was adjusted to 7.4 and the solution was incubated at 37 °C with gentle shaking for 96 h. To prepare Aβ40 fibrils with the DMPC/DMPG vesicles, lipid vesicles (2.5 mM) were added to a 100 μM Aβ40 peptide solution to give a final Aβ concentration of 50 μM and the solution was incubated at 37 °C with gentle shaking for 2 h. The pellets were collected into NMR rotors by ultracentrifugation, lyophilized, and rehydrated with 30 % water. NMR experiments were carried out on a wide-bore Varian VNMRS 600 MHz (14.1 T) NMR spectrometer with a 4 mm triple-resonance T3-HXY MAS probe and a standard bore Bruker 800 MHz (18.8 T) NMR spectrometer with a 3.2 mm E-free HCN probe.

Received: December 21, 2013
Published online: May 8, 2014

Keywords: Alzheimer's disease · β-amyloid aggregation · magic-angle spinning · NMR spectroscopy · protein structures

[1] A. T. Petkova, R. D. Leapman, Z. H. Guo, W. M. Yau, M. P. Mattson, R. Tycko, *Science* **2005**, *307*, 262 – 265.
[2] A. T. Petkova, W. M. Yau, R. Tycko, *Biochemistry* **2006**, *45*, 498 – 512.
[3] A. K. Paravastu, R. D. Leapman, W. M. Yau, R. Tycko, *Proc. Natl. Acad. Sci. USA* **2008**, *105*, 18349 – 18354.
[4] I. Bertini, L. Gonnelli, C. Luchinat, J. F. Mao, A. Nesi, *J. Am. Chem. Soc.* **2011**, *133*, 16013 – 16022.
[5] J. X. Lu, W. Qiang, W. M. Yau, C. D. Schwieters, S. C. Meredith, R. Tycko, *Cell* **2013**, *154*, 1257 – 1268.
[6] M. Bokvist, F. Lindstrom, A. Watts, G. Grobner, *J. Mol. Biol.* **2004**, *335*, 1039 – 1049.
[7] K. Matsuzaki, *Biochim. Biophys. Acta Biomembr.* **2007**, *1768*, 1935 – 1942.
[8] E. Y. Chi, C. Ege, A. Winans, J. Majewski, G. H. Wu, K. Kjaer, K. Y. C. Lee, *Proteins Struct. Funct. Bioinf.* **2008**, *72*, 1 – 24.
[9] E. Terzi, G. Holzemann, J. Seelig, *Biochemistry* **1997**, *36*, 14845 – 14852.
[10] B. L. Kagan, R. Azimov, R. Azimova, *J. Membr. Biol.* **2004**, *202*, 1 – 10.
[11] M. F. M. Engel, L. Khemtemourian, C. C. Kleijer, H. J. D. Meeldijk, J. Jacobs, A. J. Verkleij, B. de Kruijff, J. A. Killian, J. W. M. Hoppener, *Proc. Natl. Acad. Sci. USA* **2008**, *105*, 6033 – 6038.
[12] H. Heise, W. Hoyer, S. Becker, O. C. Andronesi, D. Riedel, M. Baldus, *Proc. Natl. Acad. Sci. USA* **2005**, *102*, 15871 – 15876.
[13] J. J. Helmus, K. Surewicz, P. S. Nadaud, W. K. Surewicz, C. P. Jaroniec, *Proc. Natl. Acad. Sci. USA* **2008**, *105*, 6284 – 6289.
[14] C. Wasmer, A. Lange, H. Van Melckebeke, A. B. Siemer, R. Riek, B. H. Meier, *Science* **2008**, *319*, 1523 – 1526.
[15] J. R. Lewandowski, P. C. A. van der Wel, M. Rigney, N. Grigorieff, R. G. Griffin, *J. Am. Chem. Soc.* **2011**, *133*, 14686 – 14698.
[16] R. Tycko, *Annu. Rev. Phys. Chem.* **2011**, *62*, 279 – 299.
[17] G. Comellas, L. R. Lemkau, D. H. H. Zhou, J. M. George, C. M. Rienstra, *J. Am. Chem. Soc.* **2012**, *134*, 5090 – 5099.
[18] V. Daebel, S. Chinnathambi, J. Biernat, M. Schwalbe, B. Habenstein, A. Loquet, E. Akoury, K. Tepper, H. Muller, M. Baldus, C. Griesinger, M. Zweckstetter, E. Mandelkow, V. Vijayan, A. Lange, *J. Am. Chem. Soc.* **2012**, *134*, 13982 – 13989.
[19] J. T. Nielsen, M. Bjerring, M. D. Jeppesen, R. O. Pedersen, J. M. Pedersen, K. L. Hein, T. Vosegaard, T. Skrydstrup, D. E. Otzen, N. C. Nielsen, *Angew. Chem.* **2009**, *121*, 2152 – 2155; *Angew. Chem. Int. Ed.* **2009**, *48*, 2118 – 2121.
[20] S. Chimon, M. A. Shaibat, C. R. Jones, D. C. Calero, B. Aizezi, Y. Ishii, *Nat. Struct. Mol. Biol.* **2007**, *14*, 1157 – 1164.
[21] M. Ahmed, J. Davis, D. Aucoin, T. Sato, S. Ahuja, S. Aimoto, J. I. Elliott, W. E. Van Nostrand, S. O. Smith, *Nat. Struct. Mol. Biol.* **2010**, *17*, 561 – U556.
[22] S. Parthasarathy, F. Long, Y. Miller, Y. L. Xiao, D. McElheny, K. Thurber, B. Y. Ma, R. Nussinov, Y. Ishii, *J. Am. Chem. Soc.* **2011**, *133*, 3390 – 3400.
[23] J. M. Lopez del Amo, M. Schmidt, U. Fink, M. Dasari, M. Fandrich, B. Reif, *Angew. Chem.* **2012**, *124*, 6240 – 6243; *Angew. Chem. Int. Ed.* **2012**, *51*, 6136 – 6139.
[24] R. Tycko, R. B. Wickner, *Acc. Chem. Res.* **2013**, *46*, 1487 – 1496.
[25] H. A. Scheidt, I. Morgado, D. Huster, *J. Biol. Chem.* **2012**, *287*, 22822 – 22826.
[26] D. S. Wishart, B. D. Sykes, F. M. Richards, *Biochemistry* **1992**, *31*, 1647 – 1651.
[27] S. Luca, D. V. Filippov, J. H. van Boom, H. Oschkinat, H. J. M. de Groot, M. Baldus, *J. Biomol. NMR* **2001**, *20*, 325 – 331.
[28] Y. Shen, F. Delaglio, G. Cornilescu, A. Bax, *J. Biomol. NMR* **2009**, *44*, 213 – 223.
[29] C. D. Schwieters, J. J. Kuszewski, N. Tjandra, G. M. Clore, *J. Magn. Reson.* **2003**, *160*, 65 – 73.
[30] W. Qiang, W. M. Yau, Y. Q. Luo, M. P. Mattson, R. Tycko, *Proc. Natl. Acad. Sci. USA* **2012**, *109*, 4443 – 4448.
[31] F. Tofoleanu, N. V. Buchete, *J. Mol. Biol.* **2012**, *421*, 572 – 586.

